GeoConvention 2015
GEOSCIENCE
new horizons
Telus Convention Centre • 4-8 May 2015 • Calgary, AB Canada

AVA from prestack 3D VSP images

W. Scott Leaney
Schlumberger

Summary

While walkaways have been used to measure AVO for a long time (Coulombe *et al*., 1991; Leaney, 1994) and elastic properties have been recovered by inversion under an assumption of lateral invariance (Malinverno and Leaney, 2005), the recovery of elastic properties away from the well has remained elusive due to the limited angular illumination provided by the typical multi-offset VSP geometry. Previous work on using walkaway VSPs for pre-stack elastic inversion (Ahmad *et al*., 2012) made use of a 2D assumption and wavefield extrapolation to mimic a surface seismic geometry (e.g. Fuller and Sterling, 2008) but such approaches break down in 3D (Du *et al*., 2014). The advent of elastic full waveform inversion (Podgornova *et al*., 2013), however promising, is presently only 2D and computationally expensive so an efficient process to recover elastic properties from 3D VSPs is needed.

Historically, all shots and receivers in VSP migration have been stacked under an acoustic approximation (e.g. Miller *et al*., 1987; Dillon, 1988), thus AVA information is lost. In this paper the problem of AVA parameter estimation in multi-offset VSP imaging is studied using linear inverse theory and an algorithm that honours the true 3D VSP geometry is described that recovers information from AVA in pre-stack 3D VSP migrated images.

Overview

Figure 1 sketches the problem, depicting minimum and maximum specular incidence angle for a selected reflection point. The effect of conventional imaging is shown schematically, wherein amplitudes from a range of incidence angles are averaged leading to a bias in normal incidence reflectivity. The equation for a linearized 3-term P-p AVA regression is shown, valid for layered VTI media (Thomsen, 1993). The angle range, $\theta_{max} - \theta_{min}$ and angle centre, $(\theta_{max} + \theta_{min})/2$ vary significantly throughout the image, driven by the receiver and source geometry but also by the velocity model. To investigate further a synthetic was created containing eight isotropic layers with elastic parameters chosen to produce different classes of AVO. The walkaway geometry has 80 receivers and 161 sources. Angle centre and angle range parameters are shown for this geometry in image space in Figure 2; several aspects warrant emphasis. Directly under the receivers, angle centre and range are equal to zero, providing only normal incidence; at the image edge the angle range is zero while the angle centre is significantly positive; at intermediate image offsets both range and centre are positive, with no normal incidence. Angle range increases rapidly for reflections located just under receivers (the AVO walkaway principle), but for reflections beneath the receiver array only at intermediate image offsets is the angle range significant. This position-dependent variation in specular incidence angle illumination makes AVA regression an ill-posed inverse problem in need of position-dependent regularization.

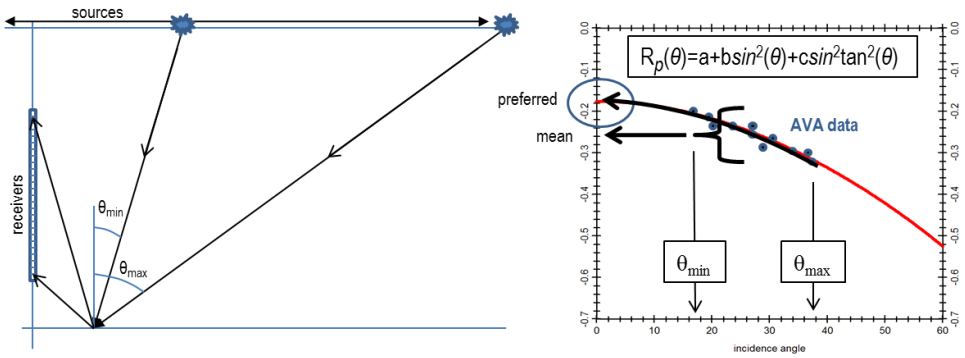

Figure 1. *Left: multi-offset VSP schematic showing minimum and maximum specular incidence angles for a selected image point; right: amplitude versus angle data with the mean as from traditional acoustic migration and the preferred intercept.*

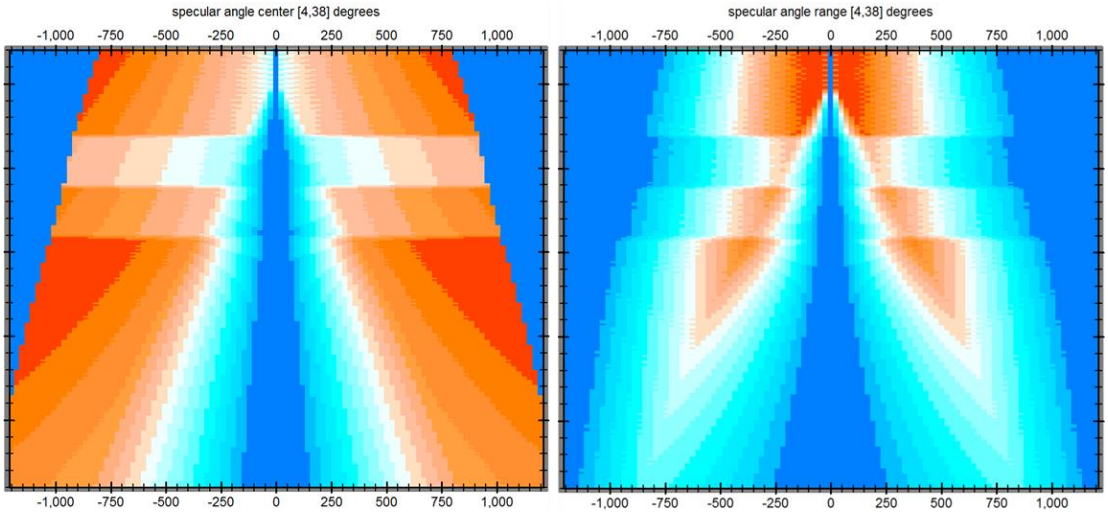

Figure 2. *Left: Specular angle center; right: specular angle range. Color scale is linear between angles [4,38] degrees = [blue,red]. The bottom of the 80-receiver array is at the top of the image.*

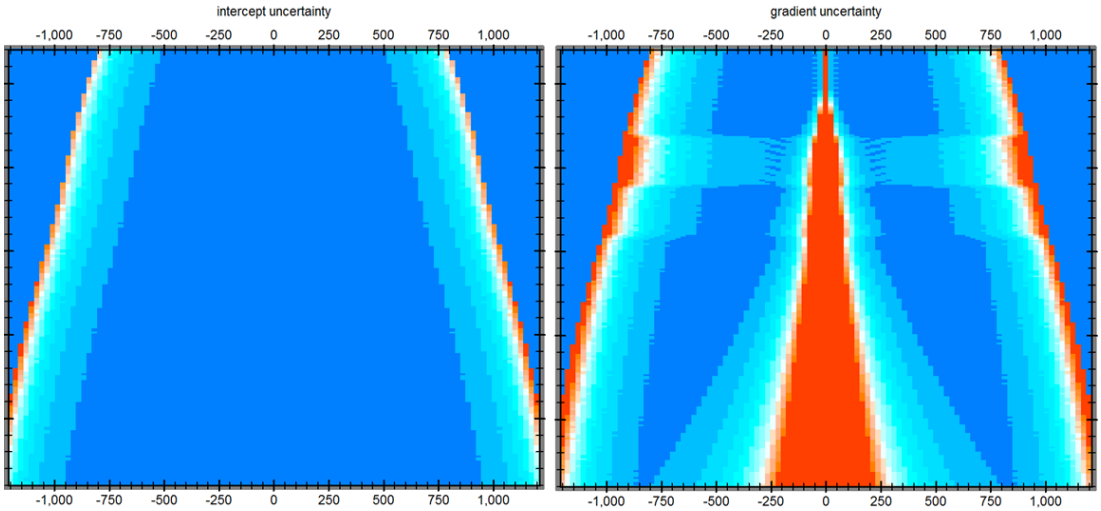

Figure 3. *Two-term AVA regression parameter uncertainties versus image point position. Left: intercept, right: gradient. The intercept is recoverable everywhere except at the image edge.*

Figure 3 shows parameter uncertainty obtained from the unit model covariance matrix (Menke, 1984) of a two-term linear regression of amplitude versus angle. The intercept term is resolved everywhere except at the image edges while the gradient term is unresolved beneath the receivers and at image edges. At zero-offset the geometry resolves only one parameter (intercept), two parameters at intermediate offsets (given sufficient signal-to-noise) and zero parameters at the image edges. Essentially, the problem is variably under-determined, necessitating dynamic regularization to provide stability while maintaining parameter resolution (e.g. Menke, 1984).

AVA regression for 3D VSP images

To accomplish AVA regression for 3DVSPs two new Omega* modules have been written. In the workflow, common receiver 3DVSP migrations are saved and incidence phase angle volumes are computed using two-point anisotropic ray tracing from receivers to image points, together with the local model dip field and Snell's Law. The migrated image and angle volumes are sorted to common image gathers and the AVA regression routine is called for every depth or time sample. This is repeated for every image gather. Volumes of AVA regression attributes are saved, including the estimated intercept, which is now an appropriate input for trace inversion to acoustic impedance. The result of applying this workflow to the synthetic data set containing several different classes of AVO is shown in Figure 4. As can be seen, the 0-offset or normal incidence reflectivity is recovered. The posterior uncertainty (Figure 3, left) can be used to mute the image edges where the intercept is not recoverable.

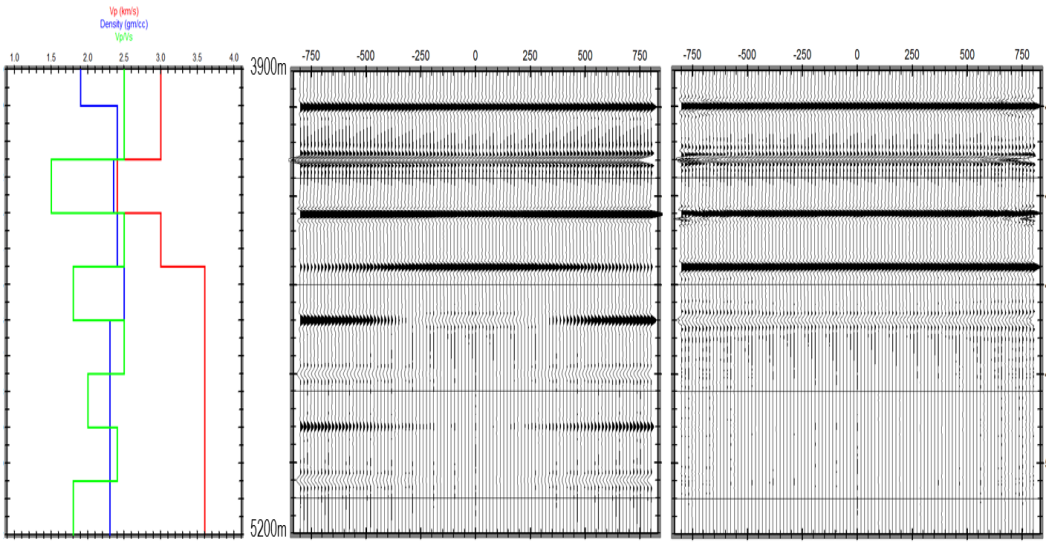

Figure 4 *Synthetic elastic model (left) showing Vp (red), density (blue) and Vp/Vs (green), specially chosen to exhibit different classes of AVO. Notice that the bottom three reflectors have zero normal incidence reflectivity. Conventional migration (middle) and the intercept term from migration followed by AVA regression (right).*

Real data application

Several important aspects need consideration when applying this approach to real data. First and foremost is the need for true amplitude common receiver migrations. This is accomplished with a careful 3C processing sequence and true-amplitude migration that includes a switch to account for the type of deconvolution that has been used. The migration may be scalar or vector (3C). Secondly, since the regression is carried out for depth or time samples in image gathers, it is important that image gathers are flat. This is accomplished with reflection tomography (Woodward *et al.*, 2008) followed by residual flattening. The application of AVA regression for 3D VSPs will be shown applied to real data in the presentation, including trace inversion of the intercept volume to acoustic impedance.

Conclusions

Quantitative 3D VSP imaging requires that AVA effects, which are always present in the data to some degree, be taken into account. The problem of AVA in multi-offset VSP imaging was analyzed with the use of a synthetic walkaway data set and linear inverse theory, showing specular incidence angle illumination and AVA parameter uncertainty. While the gradient parameter is recoverable only at intermediate image offsets, the intercept parameter is recoverable everywhere except at image edges. By computing incidence angle volumes for common receiver migrations a regression routine operating on common image gathers is able to compute AVA attributes and recover normal incidence reflectivity. The approach taken here is a rather simple, sequential one. In the future, the more sophisticated, single parameter least-squares 3DVSP migration approach (Leaney *et al*., 2009) may be extended to recover two or three parameters.

Acknowledgements

Many thanks to Wenyao Zhang and Kui Lin for coding the Omega* applications.

References

Ahmad, J., El-Marhfoul, B. and Owusu, J., 2012, Pre-stack VSP elastic inversion for lithology delineation in an offshore field of the Arabian Gulf, Saudi Arabia: EAGE Workshop, Istanbul, BG15.

Coulombe, C.A., Stewart, R.R. and Jones, M.J., 1991, AVO analysis using the VSP: *SEG Expanded Abstracts*.

Dillon, P.B., 1988, Vertical seismic profile migration using the Kirchhoff integral: *Geophysics*, **53**, 786-799.

Du, Y., Willis, M.E and Stewart, R.R., 2014, Simulating surface seismic records from VSP data: a 3D test: SEG Expanded Abstracts.

Fuller, B.N. and Sterling, J.M., 2008, Method for processing borehole seismic data: U.S. Patent 7,359,284 B2.

Leaney, W.S., 1994, Anisotropy and AVO from walkaways: *SEG Expanded Abstracts,* 105-109.

Leaney, W.S., Sacchi, M.D. and Ulrych, T.J., 2009, Least-squares migration with dip-field regularization: application to 3DVSP data: *SEG Expanded Abstracts*, 2864-2868.

Malinverno, A. and Leaney, W.S., 2005, Monte-Carlo Bayesian look-ahead inversion of walkaway vertical seismic profiles: *Geophys. Prosp.*, **53**, 689-703.

Menke, W., 1984, Geophysical Data Analysis: Discrete Inverse Theory: Academic Press, Elsevier.

Miller, D., Oristaglio, M. and Beylkin, G., 1987, A new slant on seismic imaging: migration and integral geometry: *Geophysics*, **52**, 943-964.

Podgornova, O., Leaney, S., Charara, M. and von Lunen, E., 2014, Elastic full waveform inversion for land walkaway VSP data from British Columbia: *EAGE Expanded Abstracts*.

Thomsen, L., 1993, Weak anisotropic reflections: *Offset dependent reflectivity*, Soc. Expl. Geophys., Castagna, J.P. and Backus, M.M., Eds.

Woodward, M.J., Nichols, D., Zdraveva, O., Whitfield, P. and Johns, T., 2008, A decade of tomography: *Geophysics*, **73**, No.5 ppVE5-VE11.